Time-dependent close-coupling theory for $e+$H elastic and inelastic scattering

M. C. Witthoeft, S. D. Loch, and M. S. Pindzola

Department of Physics, Auburn University, Auburn, Alabama 36849, USA

The time-dependent close-coupling theory is extended to allow the calculation of $e-$H elastic and inelastic scattering processes. We first calculate $^{1,3}S$ elastic scattering cross sections for H($1s$) in time-dependent Hartree-Fock theory and find good agreement with time-independent distorted-wave theory. We then calculate elastic scattering cross sections for H($1s$) using time-dependent close-coupling theory and find good agreement with R-matrix scattering theory. Finally, we apply the time-dependent close-coupling method to calculate elastic and inelastic cross sections for H($2s$) and H($2p$). Correlation effects are found to be important in all elastic and inelastic processes involving the $n=2$ excited states of hydrogen. In particular, the ionization cross sections are used to calculate ionization rate coefficients for comparison with rate coefficients currently used in collisional-radiative models.

I. INTRODUCTION

Electron-impact scattering on hydrogen is one of the most fundamental and important collision systems and, although frequently studied, there remains much that is not fully understood. The time-dependent close-coupling (TDCC) method has been applied with great success to the electron-impact ionization of ground state hydrogen, for both total [1] and triple differential [2] cross sections. Since the TDCC method is formulated on a lattice, a full treatment is made of both bound and continuum coupling effects. The nonperturbative TDCC results were found to differ significantly with first-order distorted-wave calculations, indicating the importance of accurately accounting for high-order electron correlation effects. Since electron correlation effects are important in elastic scattering, in addition to inelastic scattering, we extend the TDCC method to include elastic scattering, along lines somewhat different from those used by Yamanaka and Kino [3] to calculate TDCC scattering cross sections for positrons off hydrogen and helium.

We begin with a formulation for elastic scattering of electrons off hydrogen using time-dependent Hartree-Fock (TDHF) theory. This method, which is found to yield equivalent results to time-independent Hartree-Fock (TIHF) distorted-wave theory, serves as a guide in formulating a similar time-dependent close-coupling theory, where the electron correlation effects are treated to all orders. After checking the accuracy of the method for elastic scattering from the ground state with variational calculations [4], we apply the method to elastic and inelastic processes of excited states. Previous calculations of elastic scattering from H($2s$) [5–9] consist mainly of perturbative approaches valid at higher electron-impact energies ($E \geqslant 100$ eV). To our knowledge, there are no nonperturbative calculations published for elastic scattering from either $n=2$ level of hydrogen. As for ionization, Bartschat and Bray [10] have reported R-matrix with pseudostates and converged close-coupling calculations for the 2s state but there is nothing published for ionization from the 2p state. We find greater disagreement between distorted-wave theory and the present time-dependent close-

coupling method for ionization from excited states than was found for ground state ionization. This confirms the trend observed recently in nonperturbative calculations on Li [11,12] and Be [13], which has important implications in the modeling of fusion plasmas [14,15] where ionization from excited states plays an important role. These implications are demonstrated by comparing ionization rate coefficients generated from our time-dependent close-coupling calculations and distorted-wave calculations, as well as exchange classical impact parameter theory.

The rest of the paper is organized as follows. In Sec. II we derive the time-dependent Hartree-Fock equations for S-wave scattering. We then extend the time-dependent close-coupling theory in Sec. III to include elastic scattering. This new formulation of the TDCC method is applied to electron scattering off hydrogen in Sec. IV, where elastic and inelastic cross sections are calculated from the ground and $n=2$ excited states. Finally, we summarize our results in Sec. V. Unless otherwise noted, all quantities are given in atomic units.

II. $^{1,3}S$ ELASTIC SCATTERING IN TIME-DEPENDENT HARTREE-FOCK THEORY

For electron scattering from a one-electron target atom, the Hamiltonian is given by

$$H = -\frac{1}{2}\nabla_1^2 - \frac{1}{2}\nabla_2^2 - \frac{Z}{r_1} - \frac{Z}{r_2} + \frac{1}{|\vec{r}_1 - \vec{r}_2|}, \quad (1)$$

where $\vec{r}_1$ and $\vec{r}_2$ are the coordinates of the two electrons and Z is the atomic number. The total ^1S wave function in the frozen core approximation is given by

$$\psi(r_1, r_2, t) = \sqrt{\frac{1}{2}}[P_{1s}(r_1)F_{k_0 s}(r_2, t) + F_{k_0 s}(r_1, t)P_{1s}(r_2)], \quad (2)$$

where $P_{1s}(r)$ is the radial orbital for the ground state and k_0 is the linear momentum of the incident electron. From pro-

jection onto the time-dependent Schrödinger equation:

$$\int_0^\infty dr P_{1s}(r)\left(i\frac{\partial}{\partial t} - H\right)\psi(r,r',t) = 0, \tag{3}$$

we obtain the time-dependent Hartree-Fock equation:

$$i\frac{\partial F_{k_0s}(r,t)}{\partial t} = \left(-\frac{1}{2}\frac{d^2}{dr^2} - \frac{Z}{r}\right)F_{k_0s}(r,t)$$

$$+ \int_0^\infty dr' \frac{P_{1s}^2(r')}{\max(r,r')}F_{k_0s}(r,t)$$

$$+ \int_0^\infty dr' \frac{P_{1s}(r')F_{k_0s}(r',t)}{\max(r,r')}P_{1s}(r)$$

$$- \int_0^\infty dr' \int_0^\infty dr'' \frac{P_{1s}^2(r')P_{1s}(r'')F_{k_0s}(r'',t)}{\max(r',r'')}P_{1s}(r). \tag{4}$$

The second term on the right-hand side of Eq. (4) is a direct potential, the third term is an exchange potential, and the fourth term is an exchange-overlap potential arising from the nonorthogonality of the $P_{1s}(r)$ and $F_{k_0s}(r,t)$ orbitals in ^1S scattering. A similar derivation starting from the total ^3S wave function in the frozen core approximation yields:

$$i\frac{\partial F_{k_0s}(r,t)}{\partial t} = \left(-\frac{1}{2}\frac{d^2}{dr^2} - \frac{Z}{r}\right)F_{k_0s}(r,t)$$

$$+ \int_0^\infty dr' \frac{P_{1s}^2(r')}{\max(r,r')}F_{k_0s}(r,t)$$

$$- \int_0^\infty dr' \frac{P_{1s}(r')F_{k_0s}(r',t)}{\max(r,r')}P_{1s}(r). \tag{5}$$

Since the $P_{1s}(r)$ and $F_{k_0s}(r,t)$ orbitals are orthogonal in ^3S scattering, no exchange-overlap potential is found in Eq. (5).

At time $t=0$ the time-dependent radial orbital is given by

$$F_{k_0s}(r,t=0) = \sqrt{\frac{1}{w\sqrt{\pi}}}e^{-(r-r_0)^2/2w^2}e^{-ik_0r}, \tag{6}$$

where r_0 and w are the localization radius and width of the wave packet, respectively. After time evolution of either Eq. (4) or Eq. (5) the time-dependent radial scattered orbital is constructed from

$$G_{k_0s}(r,t) = F_{k_0s}(r,t) - F_{k_0s}^{(0)}(r,t), \tag{7}$$

where $F_{k_0s}^{(0)}(r,t)$ is obtained by solution of the free-particle time-dependent Schrödinger equation, i.e.,

$$i\frac{\partial F_{k_0s}^{(0)}(r,t)}{\partial t} = -\frac{1}{2}\frac{d^2 F_{k_0s}^{(0)}(r,t)}{dr^2}. \tag{8}$$

For scattering from the neutral hydrogen atom (with $Z=1$), the total $L=0$ elastic cross section is given by

TABLE I. Electron-impact total elastic cross sections for hydrogen for S-wave scattering with an electron-impact energy of 50 eV ($1.0 \text{ Mb} = 1.0 \times 10^{-18} \text{ cm}^2$).

Case	TDHF (Mb)	TIHF (Mb)
Hartree S	40.2	40.5
Hartree-Fock ^1S	24.2	25.4
Hartree-Fock ^3S	55.1	54.5

$$\sigma = \frac{\pi}{k_0^2}\sum_k \left|\int_0^\infty dr P_{ks}^{(0)}(r)G_{k_0s}(r,T)\right|^2, \tag{9}$$

where $P_{ks}^{(0)}(r)$ are solutions of the free-particle time-independent radial Schrödinger equation over a range of linear momenta; in this case spherical Bessel functions.

We tested the time-dependent Hartree-Fock elastic scattering formalism by solving for cross sections at an incident electron energy of 50 eV. A 150 point grid from 0.0 to 30.0 was spanned by a uniform mesh with spacing $\Delta r = 0.2$. Wave packets were propagated until cross section convergence at $T=16.0$. The time-dependent elastic cross-section results are presented in column two of Table I, where they are compared with results in column three from standard time-independent scattering theory [16]. The column three results are obtained by integration of the continuum Hartree-Fock equations to find phase shifts, and thus cross sections. The Hartree S-wave results are found by wave packet propagation of Eq. (5) after dropping the exchange potential. Reasonable agreement is found between the time-dependent results and standard time-independent scattering theory.

III. ELASTIC AND INELASTIC SCATTERING IN TIME-DEPENDENT CLOSE-COUPLING THEORY

As the time-dependent close-coupling theory has been derived in detail before [17] we will only outline the method here in the process of adding the capability to extract the elastic scattering cross section from the time-propagated radial wave function. The Hamiltonian is the same as given in Eq. (1) but we expand the time-dependent wave function in terms of coupled spherical harmonics,

$$\Psi(\vec{r_1},\vec{r_2},t) = \sum_{l_1l_2}\frac{P_{l_1l_2}^{LS}(r_1,r_2,t)}{r_1r_2}\sum_{m_1m_2}C_{m_1m_20}^{l_1l_2L}Y_{l_1m_1}(\hat{r_1})Y_{l_2m_2}(\hat{r_2}), \tag{10}$$

where L and S are the total orbital and spin angular momenta of the system, $Y_{lm}(\hat{r})$ is a spherical harmonic, and $C_{m_1m_2m_3}^{l_1l_2l_3}$ is a Clebsch-Gordan coefficient. Using this wave function in the time-dependent Schrödinger equation and integrating out the angular variables, we obtain the following set of time-dependent close-coupled partial differential equations governing the behavior of the two-dimensional radial wave function,

$$i\frac{\partial P^{LS}_{l_1 l_2}(r_1,r_2,t)}{\partial t} = T_{l_1 l_2}(r_1,r_2)P^{LS}_{l_1 l_2}(r_1,r_2,t)$$

$$+ \sum_{l_1' l_2'} V^L_{l_1 l_2, l_1' l_2'}(r_1,r_2)P^{LS}_{l_1' l_2'}(r_1,r_2,t), \quad (11)$$

where $T_{l_1 l_2}(r_1,r_2)$ contains the kinetic energy, centrifugal barrier, and nuclear potential terms and $V^L_{l_1 l_2, l_1' l_2'}(r_1,r_2)$ is a coupling operator arising from the interaction potential between the active electrons in the Hamiltonian.

The initial time wave function is constructed as a product function of a bound radial orbital and an incoming Gaussian wave packet that is not initially symmetrized according to the total spin S. For example, when the target electron is initially in the $2p$ state the initial time wave function is

$$P^L_{pl}(r_1,r_2,t=0) = P_{2p}(r_1)g_{kl}(r_2), \quad (12)$$

where $g_{kl}(r)$ is the Gaussian wave packet with linear momentum k and angular momentum l that represents the incident electron. For each partial wave, the angular momentum of the incident electron, l, is chosen so that the total angular momentum is L. Note that when both the angular momentum of the target electron and the total angular momentum are greater than zero, l can take multiple values and a separate calculation is required for each. After the initial wave function is time evolved for a sufficient time, $t=T$, so that the transition probabilities are converged, we construct an unsymmetrized radial scattered orbital as

$$G^L_{l_1 l_2}(r_1,r_2,t) = P^L_{l_1 l_2}(r_1,r_2,t) - P^{(0)}_{l_1 l_2}(r_1,r_2,t), \quad (13)$$

where $P^{(0)}_{l_1 l_2}(r_1,r_2,t)$ is obtained by solving the following differential equation simultaneously with Eq. (11),

$$i\frac{\partial P^{(0)}_{l_1 l_2}}{\partial t}(r_1,r_2,t) = \left(-\frac{1}{2}\frac{d^2}{dr_1^2} + \frac{l_1(l_1+1)}{2r_1^2} - \frac{1}{2}\frac{d^2}{dr_2^2} + \frac{l_2(l_2+1)}{2r_2^2}\right.$$
$$\left. - \frac{Z}{r_1}\right)P^{(0)}_{l_1 l_2}(r_1,r_2,t). \quad (14)$$

Continuing with our example of the target electron being in the $2p$ state, the elastic scattering cross section, after spin averaging, is

$$\sigma_{\text{elastic}} = \frac{\pi}{4k_0^2}\sum_{LS}(2L+1)(2S+1)$$

$$\times \sum_k \left|\int_0^\infty dr_1 \int_0^\infty dr_2 G^{LS}_{1l}(r_1,r_2,T)P_{2p}(r_1)P^{(0)}_{kl}(r_2)\right|^2, \quad (15)$$

where k_0 is the initial linear momentum of the incident electron, $G^{LS}_{l_1 l_2}(r_1,r_2,t)$ is the radial scattered orbital now symmetrized according to the total spin of the system, and $P^{(0)}_{kl}(r)$ are one-electron solutions of the free particle Schrödinger equation, which are analogous to the $F^{(0)}_{k_0 s}(r)$ in the last section.

TABLE II. Electron-impact total elastic cross sections for ground state hydrogen using time-dependent close-coupling theory compared to an intermediate energy R-matrix calculation and time-independent Hartree-Fock theory with an electron-impact energy of 30.6 eV (1.0 Mb$=1.0\times10^{-18}$ cm^2).

Case	TDCC (Mb)	R-matrix, Scholz et al. [4] (Mb)	TIHF (Mb)
^1S	11.3	11.2	38.0
^3S	86.4	86.1	114.7
^1P	2.3	2.1	0.0
^3P	54.6	52.9	56.8
^1D	2.6	2.5	0.0
^3D	11.3	10.8	8.1

IV. TIME-DEPENDENT CLOSE-COUPLING RESULTS

Our time-dependent close-coupling calculations for electron-impact scattering of ground and excited state hydrogen are performed on a 384×384 point grid with a lattice spacing of 0.2 a.u. This radial lattice supports spectroscopic orbitals up to $n=4$, and the $2s$ and $2p$ ionization energies on the lattice are -3.3930 and -3.4043 eV, respectively, which are close to the true value of -3.4015 eV.

A. Elastic scattering from ground state hydrogen

As elastic scattering from the ground state of hydrogen is well understood, we present results using the TDCC method at just a single energy in order to compare with the intermediate energy R-matrix results of Scholz et al. [4]. The calculations are performed with an electron impact energy of 30.6 eV on the grid described above. The results, presented per partial wave in Table II for $L=0$, 1, 2, are in good agreement with those of Scholz et al. Also included in the table are time-independent Hartree-Fock calculations, where the $L=0$ partial wave is found to be in fairly large disagreement with our results and the R-matrix calculations. We have also calculated the elastic cross sections at $L=3$, 4 using the TDCC method in order to get a total elastic cross section of $\sigma_{\text{elastic}}=178.6$ Mb which is in good agreement with the coupled-channel optical calculation by Bray et al. [18]. Given the good agreement of our results with other nonperturbative calculations, we can now apply, with confidence, the time-dependent close-coupling theory to elastic and inelastic scattering of excited states.

B. Elastic and inelastic scattering from excited state hydrogen

We perform the excited state calculations at three electron-impact energies between two and five times the ionization threshold. We are concerned with this energy range since it is where we have found the greatest discrepancy between previous nonperturbative calculations of excitation and ionization processes and distorted-wave theory [1]. Due to computational constraints, we only run the time-dependent close-coupling calculation up to $L=8$ and approximate the larger partial wave contributions using techniques to be described.
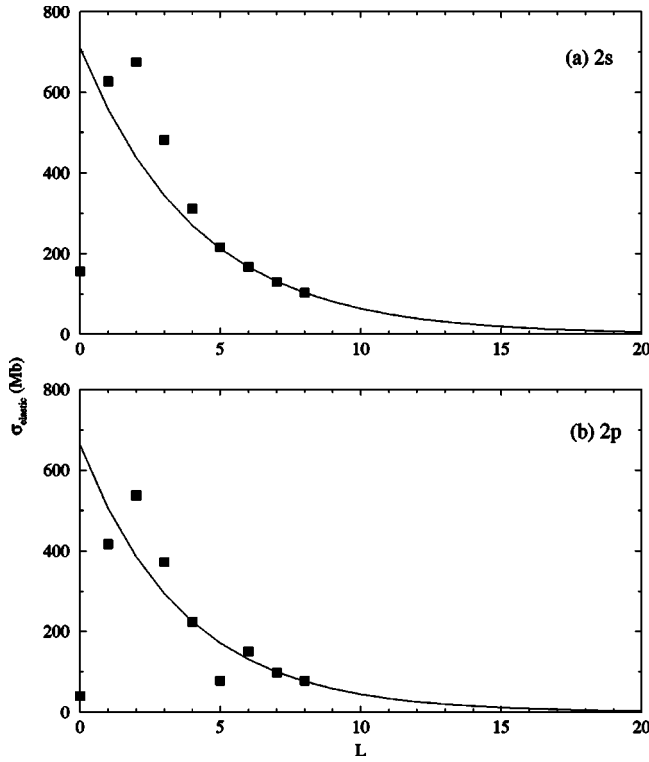
FIG. 1. Elastic scattering cross sections per partial wave for (a) H(2s) and (b) H(2p) with an electron-impact energy of 16 eV. The filled squares are the time-dependent close-coupling results and the solid curve is the fit used to approximate the cross section at large L. The cross section is given in Mb (1 Mb=10^{-18} cm^2).

TABLE III. Elastic scattering cross sections for both $n=2$ states of hydrogen using time-dependent close-coupling theory (1.0 Mb $=1.0\times10^{-18}$ cm^2).

Energy (eV)	σ_{2s} (Mb)	σ_{2p} (Mb)
8	5970	3390
12	4160	2250
16	3150	1680

error in the extrapolation should not affect the total cross section significantly. Our values of the total elastic scattering cross section from both excited states are shown in Table III.

As was the case for elastic scattering, we also need to extrapolate the ionization cross section to large values of L. For these calculations we use configuration average distorted-wave theory with a postform scattering potential to provide the $L>8$ contribution in a manner that has been described before [11,12]. The postform scattering potential refers to the method where all the electrons are solved in a V^{N-1} potential [19] as opposed to the prior form where the incident and scattered electrons are solved in a V^N potential while the bound and ionized electrons are solved in a V^{N-1} potential [20]. Within the distorted-wave approximation, there is about a 20% variability in the ionization cross sections depending on the choice of the scattering potential. For this system, the total ionization cross section from the postform distorted-wave calculations are also in better agreement with our time-dependent calculations than the prior form distorted-wave calculations. The distorted-wave calculations are also useful to compare our total ionization cross sections against, as their accuracy is representative of the data being used in current fusion plasma models.

For the case of ionization, we are not only interested in the cross section, but also the ionization rate coefficient, as this is an important quantity in collisional-radiative models. Calculation of the rate coefficient involves a convolution of the ionization cross section with a Maxwellian free electron distribution. As time-dependent close-coupling calculations are computationally intensive, especially for excited state systems, we choose to perform the calculations for only three electron-impact energies near the peak of the cross section. Once the peak is determined, we then use an analytic parameterized formula by Rost and Pattard [21] to obtain a full energy-resolved cross section with the correct Wannier threshold behavior. Use of the parameterized formula requires knowing only the ionization threshold and the location and magnitude of the peak of the cross section. The parameterized formula does not have the correct high energy behavior but, in determining the rate coefficient in the collisional ionization region, the important areas of the cross section are those up to the peak. If necessary, a fit to either the post- or prior form distorted wave at large energies will supply the correct high energy limit.

We start our analysis with ionization of H(2s) as there has been much work done on this system. In Fig. 2, we show the time-dependent close-coupling calculation as filled squares and the Rost parameterized formula using a peak location of 9.7 eV as the dashed curve. Also shown in the figure is an

Starting first with elastic scattering, we find that the elastic scattering cross section per partial wave is found to decrease more slowly for the excited states than was the case from the ground state. This is shown, for both excited state calculations, in Fig. 1 for an electron-impact energy of 16 eV. The filled squares are our time-dependent close-coupling calculations and the solid curve is the fit to our results which provides the large L contribution of the elastic scattering cross section. Since the data appear to tend to zero exponentially, we use a fitting function of the form

$$f(L)=Ae^{-bL}, \quad (16)$$

where A and b are varied to provide the best fit to our data points for the last four or five partial waves. For H(2s), shown in Fig. 1(a) for an incident electron energy of 16 eV, the elastic cross section decays regularly for $L=5-8$ giving us a good amount of confidence in our extrapolation and, in any case, the contribution to the total elastic scattering cross section for $L>8$ partial waves is only 12%. The extrapolation procedure for H(2p) elastic scattering is more complicated as the elastic cross section with $L=5$ is depressed, an effect that is found to increase with electron impact energy. This effect is shown for an incident energy of 16 eV in Fig. 1(b). The extrapolation to high-L in this example is done as in the H(2s) case but we leave out the $L=5$ and $L=6$ data points when varying the fitting parameters. As the contribution to the elastic cross section is only 11% at 16 eV, any
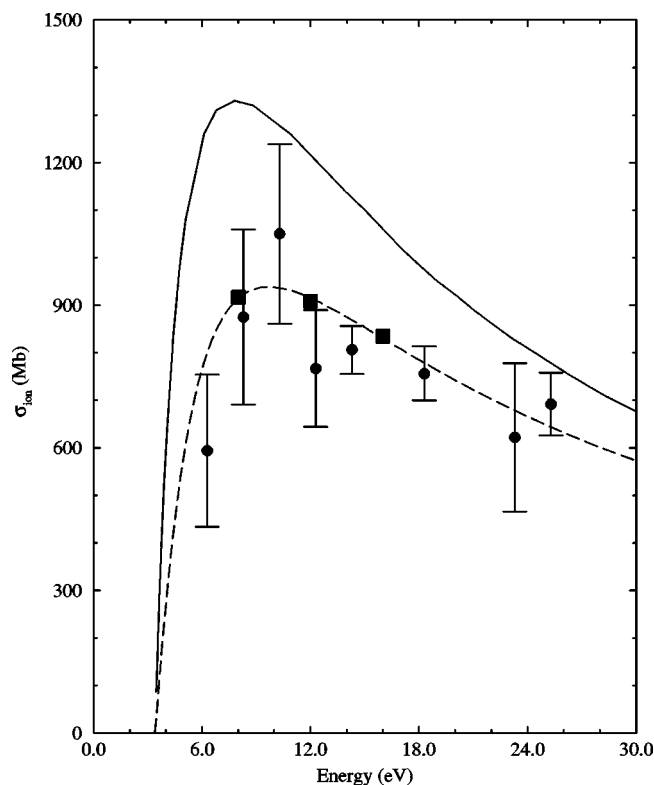
FIG. 2. Ionization cross section of H(2s) as a function of energy in eV. The filled squares are our time-dependent close-coupling results, the solid curve is a postform distorted-wave calculation, the dashed curve is a fit to the time-dependent results using the parameterized formula of Rost and Pattard [21], and the filled circles are experimental measurements by Defrance *et al.* [22]. The cross section is given in Mb (1 Mb$=10^{-18}$ cm^2).
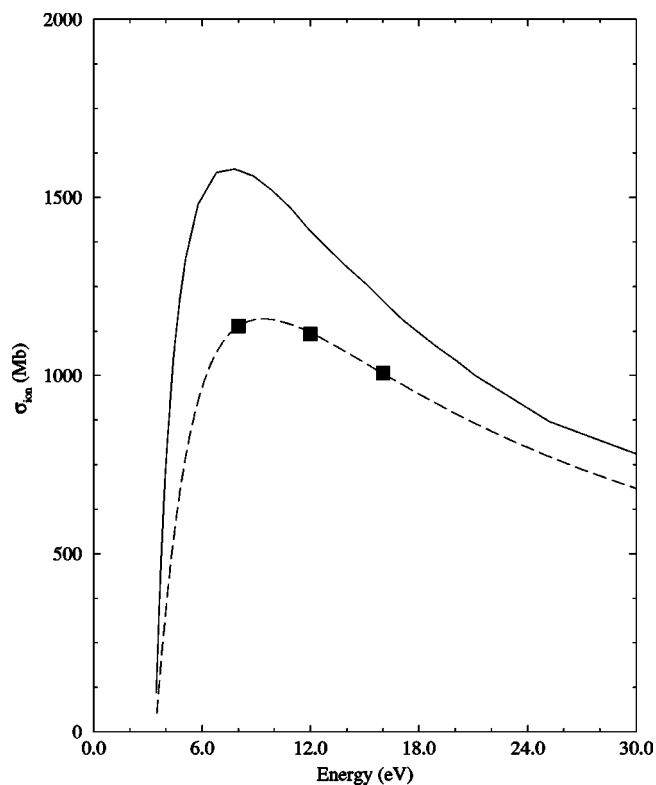

FIG. 3. Ionization cross section of H(2p) as a function of energy in eV. The filled squares are our time-dependent close-coupling results, the solid curve is a postform distorted-wave calculation, and the dashed curve is a fit to the time-dependent results using the parameterized formula of Rost and Pattard [21]. The cross section is given in Mb (1 Mb$=10^{-18}$ cm^2).

experiment by Defrance *et al.* [22] as the filled circles and a postform distorted-wave calculation as the solid curve. The percentage contribution to the total ionization cross section from $L > 8$, supplied by a fit to the postform distorted-wave calculation, is around 30% leading us to expect that our ionization results are good at the 10% level. R-matrix with pseudostates and converged close-coupling calculations by Bartschat and Bray [10] have also been performed for this system as well as an experiment by Dixon [23] but, as these results are in good agreement with the present calculation and the experiment by Defrance *et al.*, they are not shown in the figure. For neutral systems, distorted-wave theory has been found to overestimate the ionization cross section at energies near the ionization threshold, see, for example, [1,11], and the same behavior is found here as the peak of the distorted-wave cross section is about 45% higher than our time-dependent close-coupling results. Previous time-dependent close-coupling calculations for ionization from ground state hydrogen [1] found that the distorted-wave cross section was about 15% too large at the peak. The fact that the distorted wave performs worse for the excited state ionization confirms the trend found in previous nonperturbative calculations [11–13], as discussed in the Introduction. These same features are also observed for ionization from H(2p), which is shown in Fig. 3. Besides our time-dependent close-coupling results, given as filled squares, we show the

Rost parameterized formula with a peak energy of 9.4 eV as the dashed curve and a postform distorted-wave calculation as the solid curve. The distorted-wave calculation is about 40% higher at the peak than the present time-dependent calculation which is the same level of accuracy that was found with ionization from the 2s state.

The most critical values of the ionization rate coefficient are especially sensitive to the behavior of the ionization cross section at energies near the ionization threshold. As can be seen from Figs. 2 and 3, the slope of the cross section from the threshold is different for our calculations and the postform distorted-wave calculation, which results in large differences in the rate coefficients. This can be seen in Fig. 4 where the ratio of the postform distorted-wave rate coefficient to our time-dependent close-coupling rate is plotted as the thin solid curve for ionization from H(2s) and the thick solid curve is H(2p). Also included in the figure are the ratios of a rate using the exchange classical impact parameter (ECIP) method to our time-dependent calculations; the thin dashed curve is for H(2s) and the thick dashed curve is H(2p). The ECIP method [14] is a classical plus impact-parameter approach used in current collisional-radiative models [25] to provide ionization data for excited state systems where no accurate nonperturbative data exist. Ionization of hydrogen becomes appreciable in a plasma for electron temperatures roughly around a tenth of the ionization
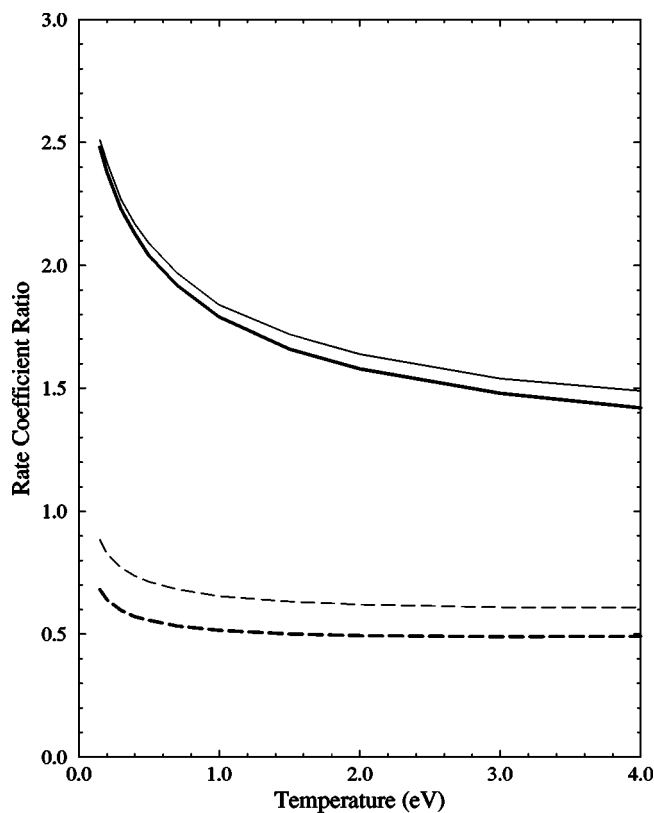
FIG. 4. Ratio of postform distorted-wave and exchange classical impact parameter calculations to the present time-dependent close-coupling calculations for both $n=2$ excited states of hydrogen as a function of electron temperature in eV. The thin solid curve and thick solid curve are the distorted-wave ratios for H(2s) and H(2p), respectively, and the thin dashed curve and thick dashed curve are the exchange classical impact parameter ratios for H(2s) and H(2p).

threshold and virtually all of the hydrogen is ionized for temperatures exceeding the ionization threshold. Given those limits, we see that the postform distorted-wave calculations are most accurate at the larger electron temperatures but, even at these larger temperatures, are still about 50% larger than the present calculations for both 2s and 2p excited states. The ECIP results for H(2s) underestimate the ionization rate between 30% and 40% over the temperture range of

interest, whereas the results for H(2p) are about 50% lower than the present calculation. It must be noted that the ECIP rate coefficients depend only on the ionization threshold, meaning that the actual ECIP rate coefficients for H(2s) and H(2p) are the same. The difference between the ECIP to time-dependent close-coupling rate ratios for 2s and 2p is due entirely to the difference in the time-dependent calculations for the two excited state systems.

The time-dependent close-coupling data are available through Oak Ridge National Laboratory's Controlled Fusion Atomic Data Center (CFADC) [24] and the Atomic Data and Analysis Structure (ADAS) database [25].

V. SUMMARY

We have derived time-dependent Hartree-Fock equations for S-wave elastic scattering and found good agreement with a standard time-independent method. The time-dependent close-coupling theory was then extended to include the calculation of elastic scattering cross sections. A test of the theory was made for elastic scattering of electrons off ground state hydrogen that was found to be in good agreement with an intermediate energy R-matrix calculation. We then presented elastic scattering and ionization cross sections for H(2s, 2p) at three energies between two and five times the ionization threshold. Good agreement is found between the present time-dependent close-coupling calculations and previous nonperturbative calculations and experiments where they exist. Furthermore, we find that the ionization rate coefficients predicted by the exchange classical impact parameter method are a factor of 2 lower than the present calculations for H(2p), whereas postform distorted-wave calculations vary between 50% and 100% too large over the important temperature range. Areas of future work include using the time-dependent close-coupling method to calculate differential elastic cross sections for atoms and their ions.

ACKNOWLEDGMENTS

[1] M.S. Pindzola and F. Robicheaux, Phys. Rev. A **54**, 2142 (1996).

[2] J. Colgan, M.S. Pindzola, F.J. Robicheaux, D.C. Griffin, and M. Baertschy, Phys. Rev. A **65**, 042721 (2002).

[3] N. Yamanaka and Y. Kino, Phys. Rev. A **68**, 052715 (2003).

[4] T. Scholz, P. Scott, and P.G. Burke, J. Phys. B **21**, L139 (1988).

[5] C.J. Joachain, K.H. Winters, L. Cartiaux, and R.M. Mendez-Moreno, J. Phys. B **10**, 1277 (1977).

[6] C.J. Joachain and K.H. Winters, J. Phys. B **13**, 1451 (1980).

[7] S.S. Tayal, Phys. Rev. A **28**, 2535 (1983).

[8] S. Vucic, R.M. Potvliege, and C.J. Joachain, J. Phys. B **20**, 3157 (1987).

[9] T.S. Ho and F.T. Chan, Phys. Rev. A **17**, 529 (1978).

[10] K. Bartschat and I. Bray, J. Phys. B **29**, L577 (1996).

[11] D.C. Griffin, D.M. Mitnik, J. Colgan, and M.S. Pindzola, Phys. Rev. A **64**, 032718 (2001).

[12] M. Witthoeft, J. Colgan, M.S. Pindzola, C.P. Ballance, and D.C. Griffin, Phys. Rev. A **68**, 022711 (2003).

[13] J. Colgan, S.D. Loch, M.S. Pindzola, C.P. Ballance, and D.C. Griffin, Phys. Rev. A **68**, 032712 (2003).

[14] A. Burgess and H.P. Summers, Mon. Not. R. Astron. Soc. **174**,

345 (1976).

[15] S.D. Loch, M.S. Pindzola, C.P. Ballance, D.C. Griffin, D.M. Mitnik, N.R. Badnell, M.G. O'Mullane, H.P. Summers, and A.D. Whiteford, Phys. Rev. A **66**, 052708 (2002).

[16] H. P. Kelly, Phys. Rev. **171**, 54 (1968).

[17] M.S. Pindzola and D.R. Schultz, Phys. Rev. A **53**, 1525 (1996).

[18] I. Bray, D.A. Konovalov, and I.E. McCarthy, Phys. Rev. A **43**, 5878 (1991).

[19] J.H. Macek and J. Botero, Phys. Rev. A **45**, R8 (1992).

[20] S.M. Younger, Phys. Rev. A **22**, 111 (1980).

[21] J.M. Rost and T. Pattard, Phys. Rev. A **55**, R5 (1997).

[22] P. Defrance, W. Claeys, A. Cornet, and G. Poulaert, J. Phys. B **14**, 111 (1981).

[23] A.J. Dixon, A. von Engel, and M.F.A. Harrison, Proc. R. Soc. London, Ser. A **343**, 333 (1975).

[24] http://www-cfadc.phy.ornl.gov/data_and_codes

[25] http://adas.phys.strath.ac.uk